2000M&PS...35.1109S

Meteoritics & Planetary Science 35, 1109–1115 (2000)
© Meteoritical Society, 2000. Printed in USA.

New type of radiation of bright Leonid meteors above 130 km

PAVEL SPURNÝ[1]* , HANS BETLEM[2], KLAAS JOBSE[2], PAVEL KOTEN[1] AND JAAP VAN'T LEVEN[2]

[1]Astronomical Institute, Ondrejov Observatory, 251 65 Ondrejov, Czech Republic
[2]Dutch Meteor Society, Lederkarper 4, 2318 NB Leiden, The Netherlands
*Correspondence author's e-mail address: spurny@asu.cas.cz

(Received 2000 March 27; accepted in revised form 2000 July 11)

Abstract–In this paper, we study the extremely high beginning parts of atmospheric trajectories of seven Leonid meteors recorded by sensitive TV systems equipped with image intensifiers up to apparent magnitude +6.5. For all seven cases, we observed comet-like diffuse structures with sizes on the order of kilometers that developed quickly during the meteoroids' descent through the atmosphere. For the brightest event with a maximum absolute magnitude of –12.5, we observed an arc similar to a solar protuberance and producing a jet detectable several kilometers sideways from the brightest parts of the meteor head, and moving with a velocity over 100 km/s. These jets are common features for the seven studied meteors. Precise position in trajectory, velocity, and brightness at each point is available for all seven meteors, because of double-station records on 85 km base-line. When these meteoroids reached 130 km height, their diffuse structures of the radiation quickly transformed to the usual meteor appearance resembling moving droplets, and meteor trains started to develop. These meteor phenomena above 130 km were not recognized before our observations, and they cannot be explained by standard ablation theory.

INTRODUCTION

A commonly held opinion is that the light produced by a meteoroid during its interaction with the Earth's atmosphere is only caused by the ablation process. The term ablation refers to the loss of mass of a meteoroid in the form of solid fragments or of a hot gas, which is responsible for the observed meteor phenomenon (Ceplecha *et al.*, 1998). Meteoroids entering the denser parts of atmosphere are heated up very quickly. When the surface temperature reaches ~2200 K, the meteoroid material starts to sublimate from the surface and fills the space surrounding the body with its hot vapors. Excited states of atoms of these vapors are gradually deexcited by radiation. Meteor light consists mostly of radiation of discrete emission spectral lines belonging for the most part to metals and mainly to Fe. Besides this, Leonid spectra are also very rich in atmospheric emissions of O, N, and N_2 (Borovicka *et al.*, 1999). During this ablation phase, the meteoroid gradually loses its mass and is increasingly slowing down. The Leonid meteors belong to the weakest meteoroids from all shower meteors (Spurný *et al.*, 2000) with very high entering velocities of 71 km/s. This causes the Leonid meteors to start their ablation very high and disintegrate easily in the atmosphere. The highest photographed beginning altitudes for Leonid meteors are ~130 km (Spurný *et al.*, 2000). Moreover, Fujiwara *et al.* (1998) found from video observations for two bright Leonid meteors beginning heights at altitudes of 160 km. This was confirmed in the work of Spurný *et al.* (2000) who found a strong dependence of beginning heights on the initial masses of the entering Leonid meteors (Fig. 1). The highest ever observed beginning height of a meteor was up to 200 km for the brightest meteors! However, at these altitudes, the atmospheric conditions are unfavorable to produce any detectable light at all, if we assume ablation processes as described above. The mean free path of a neutral particle is ~3 m at an altitude of 130 km, ~25 m at 160 km, and >500 m at 200 km (Champion *et al.*, 1985). At such high altitudes, there is not enough air molecules to heat and evaporate an entering meteoroid. But this radiation exists, because we observed it in rather great detail. Our observations call for some sort of an explanation different from radiation by air molecule impacts onto the surface of a meteoroid. We do not try to present any explanation in this paper, but we hope that the paper might initiate proposals explaining mechanisms of diffuse meteor radiation at very high altitudes by theoreticians of meteor phenomenon.

INSTRUMENTS AND OBSERVATIONAL SITES

All data presented in this paper have been taken during the Leonid meteor expedition to China organized by the Dutch Meteor Society in collaboration with organizers of NASA's Leonid multi-instrument aircraft campaign (MAC) (Jenniskens and Butow, 1999) in November 1998.

During the exceptional so-called "fireball night" of 1998 November 16/17, we recorded photographically >150 fireballs, but most of these were so low on the horizon that we have only single-

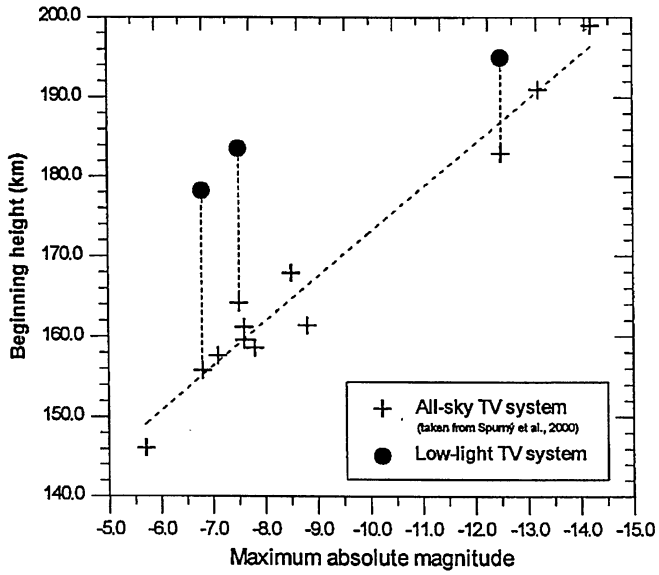

FIG. 1. Beginning heights determined from the all-sky television system as a function of maximum absolute magnitude and comparison with previously published results (Spurný *et al.*, 2000) with three Leonid meteors recorded also by the more sensitive LLTV system.

© Meteoritical Society • Provided by the NASA Astrophysics Data System

2000M&PS...35.1109S

station data. Most of the results based on photographic and all-sky video experiments have already been published (Spurný *et al.*, 2000; Betlem *et al.*, 1999).

In addition to the reported photographic efforts, we also operated a double-station video experiment with a standard Super VHS and Hi8 camcorders equipped with image intensifiers (LLTV systems). We recorded ~300 double-station meteors, data of which have not been published yet. Moreover, for seven bright events recorded photographically, we found beginning parts of their atmospheric trajectories on video records. This paper deals with these video data.

Two photographic and video stations were operated from two locations in the province of Hebei, ~150 km northeast of Beijing. The main station was located at the Xinglong Observatory, whereas the remote station was set up at Lin Ting Kou, a small village ~85 km to the south of Xinglong station.

Photographic experiments were covered by batteries of 35 mm cameras and all-sky cameras equipped with fish-eye lenses. Two batteries of 35 mm cameras of type Canon T-70 with high-quality FD 1.8/50 mm optics were placed at each observing site. This photographic system covered the sky down from ~60° from the zenith and detected meteors of visual magnitude +1 or brighter. In addition to this equipment, one all-sky photographic camera was operated at each station in order to record bright meteors (brighter then −3 magnitude) along the entire sky. These cameras were equipped with very precise F-Distagon 3,5/30 mm fish-eye objectives that enabled us to derive positions from one photograph of the whole sky hemisphere (diameter of image 80 mm) with a precision of one minute of arc or better anywhere on the picture. Such precision is comparable with the precision of 35 mm cameras equipped with 50 mm optics. The photographic cameras provided orbital and trajectory data for the brighter (larger) samples within the Leonid stream.

At Xinglong station, these photographic cameras were accompanied by an all-sky video system that was used to detect brighter meteor events and to supply the photographic experiments with the correct time of every fireball. The all-sky video system consisted of a standard Sony Hi-8 camcorder focused on the focal plane of the image intensifier Mullard XX1332 equipped with a Canon FD 2.8/15 mm fish-eye lens. The system detected meteors of magnitude +2 and brighter, so all meteors within the photographic range of meteor cameras were recorded. A more detailed description of the expedition setup are described in Spurný *et al.* (2000).

In addition to these photographic efforts, the results of which have already been reported (Betlem *et al.*, 1999; Spurný *et al.*, 2000), the Leonid 1998 expedition operated LLTV cameras at both stations that were carefully pointed to a well-defined area in the sky at ~105 km height in order to obtain double-station records of the fainter (magnitude +5 to +1) particles in the Leonid stream. The system used at the Xinglong observatory consisted of a Panasonic NV-S88E commercial video camcorder and a second-generation Russian Dedal 41 image intensifier equipped with an Arsat photographic lens 1.4/50 mm providing a field of view of 25°. According to a detailed study presented by Borovicka *et al.* (1999), this system is sensitive in the 330–880 nm range.

Similarly, the video system at the second station Lin Ting Kou consisted of the commercial Hi8 video camcorder Sony and an image intensifier Mullard XX1332 equipped with a Canon FD 1.2/85 mm aspherical objective providing a field of view of 25 × 35°. The spectral coverage is similar to a system used at Xinglong observatory, that is, 340–880 nm.

The video signal was recorded in S-VHS and Hi8 PAL system giving 25 full frames per second. A limiting sensitivity of +6.5 apparent stellar magnitude for meteors is estimated for both systems used.

OBSERVATIONAL DATA

Height Scales

When we compared photographed paths in the sky of the bright fireballs with the all-sky video images, we noted that the starting points of these fireballs were much higher in the atmosphere on the video records than on the photographic images, although the limiting magnitude for both systems was practically the same. This effect was noted for 12 cases and the all-sky video data were included in the computations with a low weight in order to get an impression of the TV beginning heights. These values were reported in Spurný *et al.* (2000), where such extremely high beginning altitudes for meteors were published for the first time.

As these values are much higher in the atmosphere than the standard aiming point for the LLTV double-station cameras, we can hardly expect to find double-station video images of very-high-starting fireballs. However, the beginning of several double-station photographed fireballs may be expected on one or the other LLTV video system.

A systematic search in the LLTV video database resulted in the finding of seven cases with a recorded beginning of a bright fireball. Only the LN98002 fireball started out of the field of view. All seven fireballs were recorded during the night of 1998 November 16/17.

The video images were measured by the semi-automated measuring software developed by Pavel Koten and they were added to the photographic sets. An accuracy of these measurements is ~2 min of arc, a factor of 3 worse than a standard reduction of a photographic 50 mm lens. Tables 1 and 2 give the results of these recomputations. Table 1 lists height intervals recorded by different methods used for observations: fish-eye camera lens (f/3.5/30 mm); 35 mm camera lens (f/1.8/50 mm), and LLTV recordings.

The LLTV beginnings are amazingly high in the atmosphere. They confirm results found with the all-sky video system and presented earlier for 12 bright Leonid meteors in Spurný *et al.* (2000). Moreover, 3 of these 12 Leonid meteors were recorded simultaneously by the LLTV system; and as this system was more sensitive than the all-sky video system, LLTV beginning altitudes were for all three common cases substantially higher as illustrated in Fig. 1. Beginning heights determined from the all-sky TV system as they depend on maximum absolute magnitude for 12 bright Leonid meteors (taken from Spurný *et al.*, 2000) are plotted in Fig. 1 and compared with those three meteors detected also by the more sensitive LLTV system. This difference is 20 km for the LN98011 fireball, 12 km for the LN98023 fireball, and 22 km for the LN98043 fireball. It is evident from Fig. 1 that at least for the brightest event recorded only by the all-sky TV system, the beginning height from the more sensitive LLTV system could be significantly higher than 200 km.

Structures in Video Images at Very High Altitudes

At very high altitudes, the early beginning of bright fireballs show a remarkable structure. Recordings of our cases start around the limiting magnitude of the LLTV systems (*i.e.*, magnitude +6). These images show a fuzzy, diffuse spot, rapidly widening and turning into a well-defined V-shape that looks remarkably like a well-developed comet with head and tail. The head is surrounded

© Meteoritical Society • Provided by the NASA Astrophysics Data System

2000M&PS...35.1109S

TABLE 1. Intervals of heights for photographic and video experiments.*

Meteor data			Intervals of heights (km) for individual observing methods				
Meteor No.	Time (UT)	M_{max}	FE	SC-X	SC-L	TV-X	TV-L
LN90002	16:36:39	–7.6	119.3–103.3	128.9–102.8	128.2–114.3	148.8–141.6	–
LN98011	18:07:43	–7.5	118.1–95.3	121.9–96.1	122.2–109.4	–	183.6–151.4
LN98013	18:25:31	–7.1	113.3–95.7	115.4–94.8	–	–	154.9–113.4
LN98023	19:33:18	–12.5	119.0–73.3	124.2–73.2	124.8–79.5	–	195.0–130.5
LN98035	20:56:10	(–6.5)	–	115.3–92.1	102.9–92.2	–	156.7–112.3
LN98036	21:10:33	(–6.5)	–	116.3–90.2	117.5–92.6	161.5–131.5	160.1–110.1
LN98043	21:42:46	–6.8	115.1–88.2	115.8–88.7	119.8–87.6	–	178.2–140.3

*M_{max} is the maximum absolute magnitude; values in parentheses are only estimates. Abbreviations: FE is the fish-eye camera at Xinglong observatory (limiting magnitude ≈ –3), SC-X are batteries of small photographic cameras (50 mm) at Xing Long observatory (limiting magnitude ≈ +1), SC-L are batteries of small photographic cameras (50 mm) at Lin Ting Kou station (limiting magnitude ≈ +1), TV-X is the low-light TV system at Xinglong observatory, and TV-L is the low-light TV system at Lin Ting Kou station.

TABLE 2. Atmospheric data from LLTV video records.

Meteor No.	H_B (km) H_E (km)	L (km)	T (s)	S (°)	R_B (km) R_E (km)	M_B M_E	H^d_B (km) H^d_E (km)	H^i_B (km) H^i_E (km)	H^s_B (km)	L_{max} (km) W_{max} (km)	H_{max} (km)
LN98002	148.8* 141.6*	29.7	0.41	13.9	150.8 149.0	4.1 2.2	148.8* 141.6*	–	–	4.2 1.2	142
LN98011	183.6 151.4*	63.5	0.88	30.3	203.5 176.0	6.1 3.3	183.6 151.4*	–	–	2.5 1.8	160
LN98013	154.9 113.4*	72.7	1.00	34.4	174.4 135.1	4.4 0.8	154.9 133	133 123	123	1.9 1.6	135
LN98023	195.0 130.5*	88.0	1.20	46.9	211.1 157.4	6.3 1.3	195.0 134	134 131*	–	5.5 3.8	148
LN98035	156.7 112.3*	50.5	0.68	61.2	170.0 138.2	5.2 1.1	156.7 135	135 125	125	2.8 1.9	138
LN98036L	160.1 110.1*	55.6	0.76	63.9	164.2 124.0	5.1 0.5	160.1 134	134 128	128	2.0 1.1	136
LN98036X	161.5 131.5*	33.4	0.48	64.0	169.2 139.8	5.6 3.0	161.5 131.5*	–	–	1.7 1.0	137
LN98043	178.2 140.3*	40.9	0.56	68.0	199.3 173.4	6.6 2.9	178.2 140.3*	–	–	1.2 1.6	145

*Not real end or beginning (edge of the field of view).

by a kind of shock-wave at an angle changing, but around 40°. When the meteors become brighter, conspicuous structures become visible in this diffuse V-tail behind the meteoroid. In almost all cases, several images clearly show visible jets and streamers. In the case of the LN98023 fireball, an arc like a solar protuberance loop is evident on at least one of the images. This is demonstrated in Fig. 2 (the reproduction might be less illustrative than the original record). This also concerns the set of frames in Fig. 3.

As all investigated cases concern double-station meteors, heights and distances for each observed point on the meteor trajectory were computed with an accuracy on the order of tens of meters. This enables us to determine the minimum displacements of the most conspicuous details. The longest jet was observed for the LN98023 meteor up to at least 7 km from the brightest point of the meteor head. It seems that the jet formed out of the meteor's head within one video frame (0.04 s) indicating an ejection velocity >100 km/s, depending on the position of its origin on the meteoroid body. Significant jets were detected also for the others meteors and their maximum lengths are 2.5 km for the LN98011 meteor, 6.5 km for the LN98036 meteor, and 3.2 km for the LN98043 meteor.

We distinguish three phases according to image appearance for these bright Leonid meteors: diffuse, intermediate, and sharp. "Diffuse image" is a widely dispersed image with very little light concentration and no clear-cut edges of the image; "sharp image" is an image of a droplet shape with sharp edges with distinct concentration of light also called meteor head; and, finally, "intermediate" image is between both of the above cases and forms for only a very short time, around a height of ~130 km when the initial diffuse image at high altitudes transforms quickly to the sharp image of normal meteor head.

We directly observed all these phases in three out of seven cases. Beginning of the intermediate phase is visible also for the 98023 fireball. The intermediate phase is visible for 0.1 to 0.2 s only, and during this period the V-shape collapses fast and the classical drop-like ablation phase becomes visible. Another common feature for all these four cases is the formation of a meteor train behind the meteor during this period. Atmospheric trajectory data for the seven fireballs for which the diffuse phase is visible are collected in Table 2. Like Table 1, the first column contains the code of the meteor. The following five columns describe the whole recorded trajectory.

© Meteoritical Society • Provided by the NASA Astrophysics Data System

2000M&PS...35.1109S

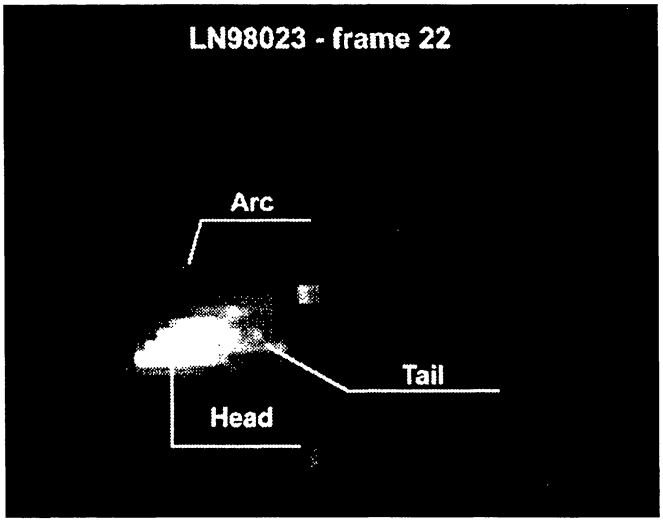

FIG. 2. The LN98023 fireball, frame 22: detection of typical diffuse structures. Field of view is 5.5 × 4.3°, altitude 150.4 km, and distance 171.0 km.

Values H_B and H_E are the beginning and terminal heights, L is the total length, T is the duration of the record, S is the slope of the atmospheric trajectory at the end point, R_B and R_E are the distances of the beginning and terminal points from the observing site, and M_B and M_E are the apparent magnitudes of the beginning and terminal points. The next three columns contain intervals of heights where the individual phases were observed. Intervals H^d_B and H^d_E describe the interval of heights where the diffuse phase was visible only, H^i_B and H^i_E describe the interval of heights of the intermediate phase, and finally, H^s_B is the height from which only the "sharp" ablation phase is visible. The following column contains the maximum observed dimensions of the diffuse tail behind the meteor head. Value L_{max} is the length along the trajectory (the distance from the brightest point in the meteor head) and W_{max} means the width perpendicular to the direction of motion at the distance L_{max}. The last column contains the value of H_{max}, which is the corresponding height where these maximum structures were observed. Table 2 shows that the diffuse structures have dimensions on the order of kilometers for all the recorded cases. We should point out that these dimensions are minimum values, because we observed each individual structure only from one observing site. Therefore we are able to determine only distances as they would be perpendicular to the line of sight.

These structures have not been reported before; only Murray *et al.* (1999) described a nebulous appearance for one bright Leonid meteor and estimated the width of their event on the order of hundred of meters.

We emphasize that instrumental effects are excluded as explanation for our cases, because meteors of the same brightness detected lower in the atmosphere with the same technique show sharp, drop-like classical ablation images regardless of their position in the field of view.

The LN98023 Fireball: A Detailed Study of the Observed Phenomenon

The LN98023 fireball is the brightest event from all of cases from which the beginnings were recorded by the LLTV technique. It reached –12.5 maximum absolute magnitude, and its picture taken by the fish-eye photographic camera at Xinglong Observatory is shown in Fig. 4. The diffuse features near the luminous trail of the fireball are caused by the long enduring train, which was visible on the all-sky video record at least 30 min after the fireball passage. This is the best case for which the diffuse phase with all types of structures was recorded by 85 mm LLTV camera at Lin Ting Kou observing site. For this reason, we will describe the evolution of the diffuse phase and individual structures observed for this extraordinary case in more detail than for the others cases. Its exceptionality consists also in the recorded range of heights and magnitudes. We have data on this fireball from the beginning altitude of 195 km down to terminal height of 73 km with a range of apparent magnitudes from +6.3 to –12.3! Basic atmospheric data for the LLTV video record are presented in Table 3. NF is the frame number, T is the corresponding time, H and R are observed height and distance, and M_{app} is the apparent magnitude. In the last column, the observed structures are described with different letters. D = diffuse appearance; C = comet-like appearance; J and A correspond to observation of jets and arcs, respectively; T = a formation of the meteor train; and I = observation of the intermediate phase.

The total length of an LLTV record is 1.20 s that corresponds to a total number of 31 frames. The meteor is partly out of the field of view on the last frame (no. 32). The fireball becomes visible on LLTV record near the center of the field of view as a faint +6.3 magnitude diffuse object. After a short and relatively steep beginning increase in brightness, a significant 0.1 s long decrease of ~1 magnitude occurred (see below). After this short but well-defined minimum of brightness (observed also for several other cases), the brightness of the meteor gradually grows and the first sign of comet-like appearance becomes visible at an altitude of 167 km. This quickly changing structure with head and tail is visible up to an altitude of 135 km, where the meteor train starts to form and the diffuse structure is gradually disappearing. On the last frame (no. 31), the diffuse phase is evidently not so dominant. Typical diffuse structures for LN98023 fireball are presented in Fig. 3, but details are not so visible as on the original record. The comet-like structure is the most developed in the interval of frames from 18 to 27, and an arc of minimum distance from the brightest part of meteor head of 2 km is visible in frame 22. At least two significant jets are detectable on the following frame 23 with a minimum distance from the brightest part of the meteor head 5.9 and 5.3 km and having significant transverse components. Let us define the XY rectangular coordinate system with its origin at the brightest point of a meteor head, and let the X axis

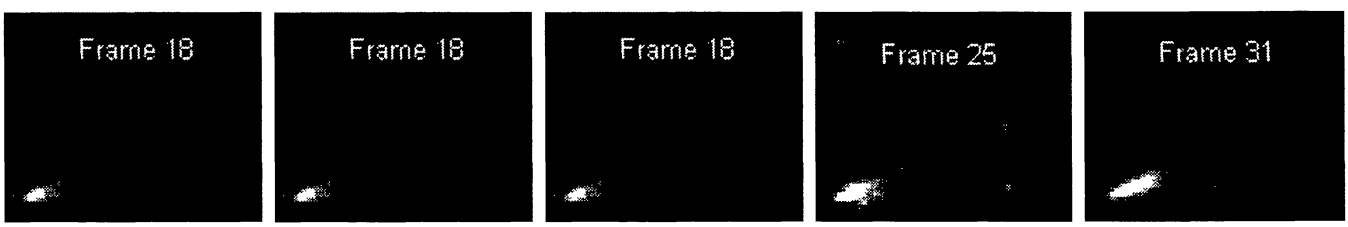

FIG. 3. Typical diffuse structures for the LN98023 fireball recorded by the LLTV system. Field of view of each frame is 6.0 × 4.8°. Altitudes and distances for individual frames are given in Table 3.

© Meteoritical Society • Provided by the NASA Astrophysics Data System

2000M&PS...35.1109S

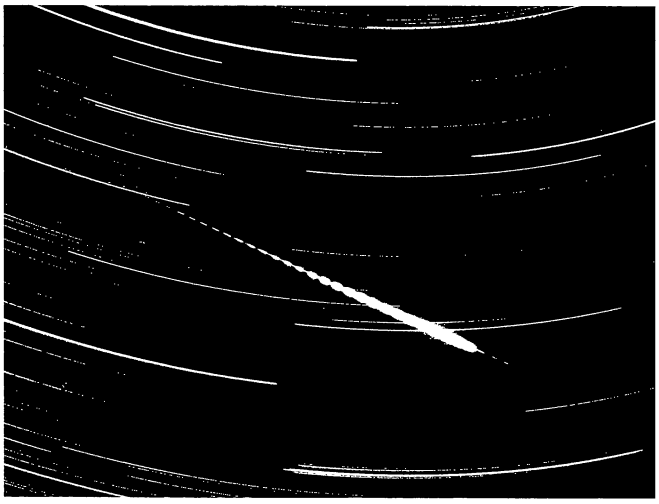

FIG. 4. The LN98023 Leonid fireball photographed by the 3.5/30 mm fish-eye camera at Xinglong observatory.

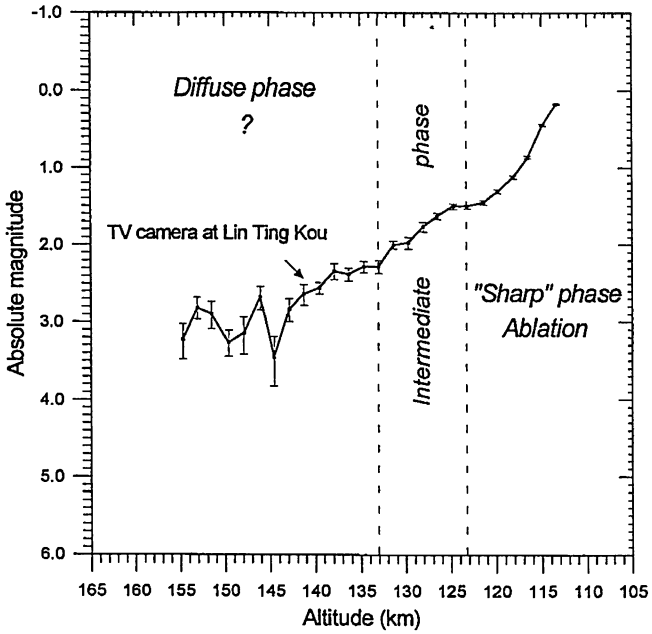

FIG. 5. Lightcurve of the LN98013 fireball.

grow in the direction of meteor radiant (opposite direction of meteor flight) and the Y axis is positive above the plane containing a meteor path and the observing location. In this coordinate system, the position of the most distant detected point on the first jet is defined with coordinates $x = 4.8$ km and $y = 3.5$ km.

Similarly, for the second jet, these coordinates are: $x = 4.8$ km and $y = 2.3$ km.

These jets were connected very probably with the arc observed in the preceding frame 22 as they were detected in the same region in respect to the meteor head. Several different jets were detected also in other frames. The longest jet was detected in frame 25 up to a minimum distance of 7 km from the brightest point of the meteor head with a transverse component of 5 km! It is very difficult to explain this observational fact and to find the mechanism that can separate material from the meteoroid so widely transverse to the motion of the meteoroid.

Light Curves of Video Records

The photometric procedure used for the determination of apparent magnitudes of meteors from video records was developed by Pavel Koten and consists of two parts. During the first part, the calibration curve is constructed; in the second part, the meteor signal is measured and a meteor brightness is determined for each frame. After dark-image subtraction, flat-fielding, and reduction, our software identifies positions of stars on the image that are used for the calibration. This operation is also useful for the computation of a meteor position. The signal of stars is determined as the summation of pixel intensities over a defined square area around the star minus background. The logarithm of this value and the catalogue magnitude is recorded for each star and the calibration curve can be computed. Similarly, the signal of the meteor is measured as the summation of intensity of corresponding pixels minus background. Finally, the apparent magnitude of the meteor is computed using the calibration curve.

The light curves based on video records are presented for all seven cases in Figs. 5–9. For practically all cases, a decrease in brightness is observed shortly after the beginning. The three cases

TABLE 3. Atmospheric data on the LLTV video record of the LN98023 fireball.

NF	T (s)	H (km)	R (km)	M_{app}	Observed structure	NF	T (s)	H (km)	R (km)	M_{app}	Observed structure
1	0.00	195.0	211.1	6.3	D	17	0.64	160.9	179.4	2.1	D,C
2	0.04	192.8	208.9	4.9	D	18	0.68	158.6	177.5	2.1	D,C
3	0.08	190.7	206.8	4.9	D	19	0.72	156.7	175.9	2.0	D,C
4	0.12	188.7	204.8	3.9	D	20	0.76	154.2	174.0	1.9	D,C
5	0.16	186.6	202.8	4.2	D	21	0.80	152.4	172.5	1.9	D,C,J
6	0.20	184.2	200.5	4.1	D	22	0.84	150.4	171.0	1.8	D,C,J,A
7	0.24	182.3	198.7	4.8	D	23	0.88	148.2	169.3	1.7	D,C,J
8	0.28	180.2	196.6	4.9	D	24	0.92	146.1	167.8	1.5	D,C,J
9	0.32	177.9	194.5	4.7	D	25	0.96	144.0	166.3	1.4	D,C,J
10	0.36	176.0	192.8	4.1	D	26	1.00	142.0	164.8	1.3	D,C,J
11	0.40	173.8	190.7	3.5	D	27	1.04	139.7	163.3	1.2	D,C,J
12	0.44	171.5	188.6	3.4	D	28	1.08	137.7	161.9	1.0	D,C,T?
13	0.48	169.4	186.8	3.1	D	29	1.12	135.6	160.6	1.0	C,T
14	0.52	167.3	184.9	2.8	D	30	1.16	133.6	159.3	0.9	C,I,T
15	0.56	165.1	183.0	2.6	D,C	31	1.20	131.7	158.0	0.8	I,T
16	0.60	163.1	181.3	2.4	D,C						

© Meteoritical Society • Provided by the NASA Astrophysics Data System

2000M&PS...35.1109S

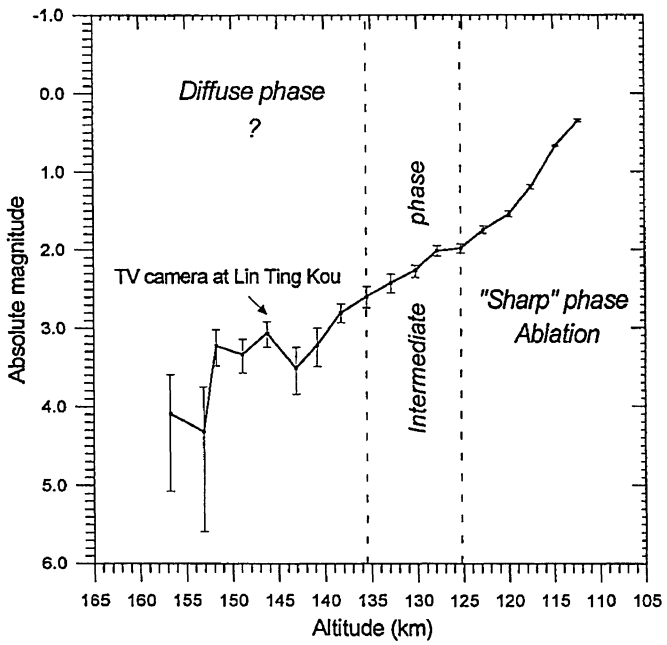

FIG. 6. Lightcurve of the LN98035 fireball.

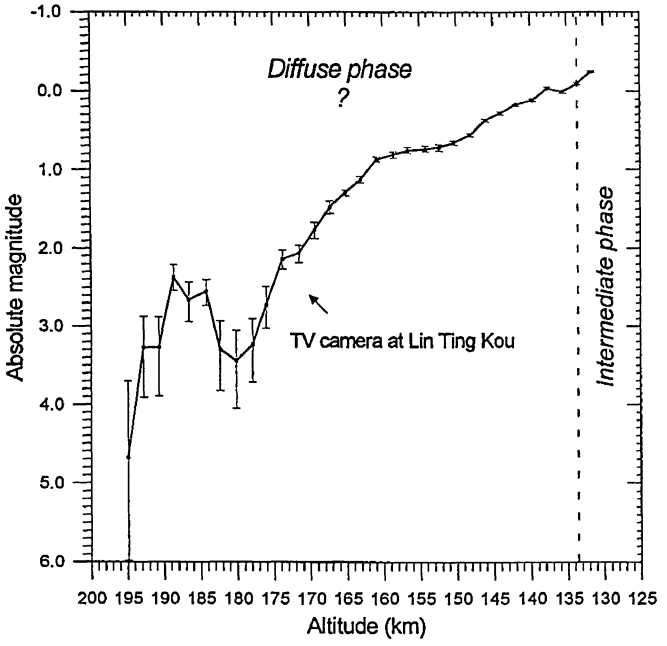

FIG. 8. Lightcurve of the LN98023 fireball.

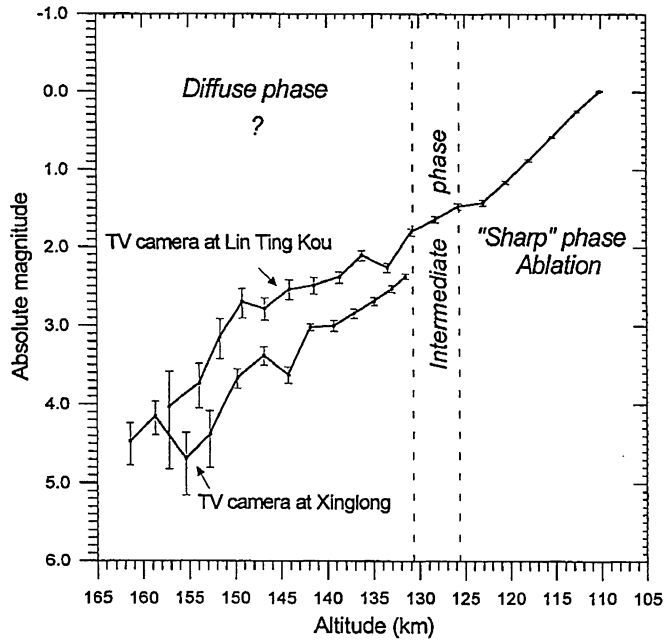

FIG. 7. Lightcurve of the LN98036 fireball.

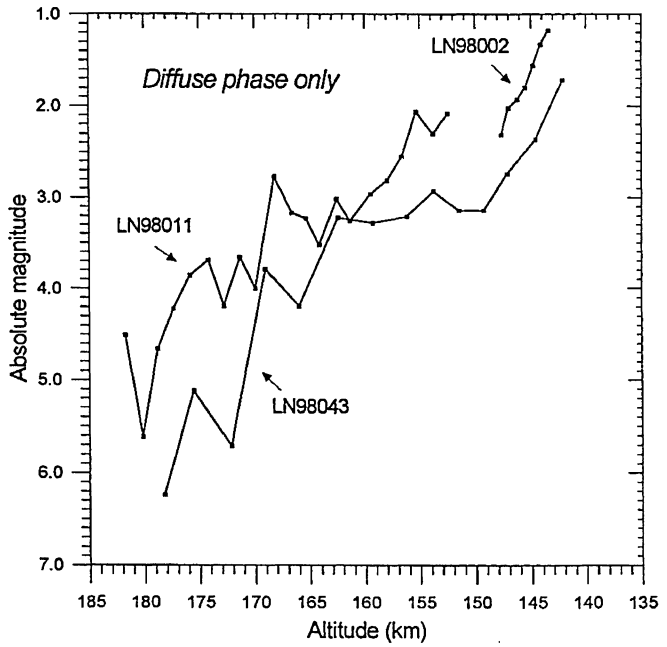

FIG. 9. Lightcurves of the LN98002, LN98011, and LN98043 fireballs.

LN98013, LN98035, and LN98036, with about the same maximum absolute magnitude (approximately –7), may be compared. Their records show a minor decrease in brightness of a half magnitude at an altitude of ~145 km (Figs. 5–7). A similar feature is shown in the case of LN98023 that was much brighter (absolute maximum magnitude –12.5) where a decrease of one magnitude is present at a height of 180 km (Fig. 8). In all cases, this decrease is ~15 km in height below the first detection of the meteor.

After the classical ablation has taken over the process, the brightness increases almost linearly with time. This early beginning of the ablation phase at an altitude of ~125 km coincides nearly with the recording limit of the classical photographic cameras.

Both the diffuse and the "sharp" ablation phases are recorded only for the three abovementioned cases. In Figs. 5–7, we can see gradually increasing brightness without any discontinuity during the intermediate phase. So far the ablation of meteors is a well known and described process, but the diffuse phase is not yet understood at all.

DISCUSSION

We confirm our previous discovery of extreme beginning heights of bright Leonids up to a height of 200 km and probably higher as all LLTV recorded beginnings are more than 10 km higher than all-sky video beginnings published in Spurný *et al.* (2000). These extremely high beginning parts of bright meteors are visible

© Meteoritical Society • Provided by the NASA Astrophysics Data System

2000M&PS...35.1109S

on video systems only. Detailed images show diffuse comet-like structures with jets. In one (the brightest) case, we detected also a well-developed arc with a minimum dimension of 2 km. Material formed in jets is ejected from the meteoroid at a very high speed and reaches distances up to the order of kilometers from the meteoroid within one video frame (0.04 s). The intermediate phase is completely recorded for three cases. Its typical duration is between 0.1 to 0.2 s, and during this period the brightness of a meteor gradually grows without any discontinuity. We observed the fast transition of a diffuse comet-like shape into a sharp drop-like shape with a parallel formation of a meteor train. It is not possible to explain the processes observed during the diffuse phase by the standard ablation model. They are very probably connected with electromagnetic processes in the upper atmosphere and with the more complicated structure of entering bodies of cometary origin. These bodies are probably composed from different kinds of material that is conserved in different layers of the initial meteoroid. We need further studies and observations to better understand these new processes connected with the early period of interaction of interplanetary bodies with the Earth's atmosphere.

Because of their diffuse apparition and possibly their spectral composition, these features were not revealed by current photographic techniques. Video shots with higher resolution of the beginnings of very bright fireballs can be obtained at rare occasions only. The 1998 Leonid fireball outburst rewarded the Dutch–Czech expedition with seven of those "lucky shots".

Acknowledgements–The authors are very grateful to all persons responsible for the organization of the 1998 Leonid expedition. Our thanks specially include those to Dr. Zhu Jin, Dr. Tan, and Dr. Xu Pin Xin from Beijing Astronomical Observatory and Purple Mountain Observatory. California Meteor Society member Ming Li helped us with translation and organization. We are also very much indebted to P. Jenniskens for his substantial support of the expedition, and we express our gratitude for helpful discussions to Z. Ceplecha and J. Borovicka. The expedition was supported by the Dutch and Chinese Academies of Sciences, the Leiden University Kerkhoven Bosscha Fund, the Dutch Physics Foundation, NASA's Planetary Astronomy Program, and NASA's Exobiology Program. The work of the Czech members of the authors' team has been partly supported by project No. K1-003-601 of the Czech Academy of Sciences and by grants of the Grant Agency of the Czech Republic Nos. 205-00-1727 and 205-99-0146.

Editorial handling: G. W. Wetherill

REFERENCES

BETLEM H. *ET AL.* (1999) Very precise orbits of 1998 Leonid meteors. *Meteorit. Planet. Sci.* **34,** 979–986.

BOROVICKA J., STORK R. AND BOCEK J. (1999) First results from video spectroscopy of 1998 Leonid meteors. *Meteorit. Planet. Sci.* **34,** 987–994.

CEPLECHA Z., BOROVICKA J., ELFORD G.W., REVELLE D.O., HAWKES R.L., PORUBCAN V. AND SIMEK M. (1998) Meteor phenomena and bodies. *Space Sci. Rev.* **84,** 327–471.

FUJIWARA Y., UEDA M., SHIBA Y., SUGIMOTO M., KINOSHITA M., SHIMODA CH. AND NAKAMURA T. (1998) Meteor luminosity at 160 km altitude from TV observations for bright Leonid meteors. *Geophys. Res. Lett.* **25,** 285–288.

JENNISKENS P. AND BUTOW S. (1999) The 1998 Leonid multi-instrument aircraft campaign. *Meteorit. Planet. Sci.* **34,** 987–994.

CHAMPION K. S. W., COLE A. E. AND KANTOR A. J. (1985) Standard and reference atmospheres. In *Handbook of Geophysics and The Space Environment* (ed. A. S. Jursa), pp. 14-1 to 14-43. Air Force Geophysics Laboratory, USA.

MURRAY I. S., HAWKES R. L. AND JENNISKENS P. (1999) Airborne intensified charge-coupled device observations of the 1998 Leonid shower. *Meteorit. Planet. Sci.* **34,** 949–958.

SPURNÝ P., BETLEM H., VAN'T LEVEN J. AND JENNISKENS P. (2000) Atmospheric behavior and extreme beginning heights of the thirteen brightest photographic Leonid meteors from the ground-based expedition to China. *Meteorit. Planet. Sci.* **35,** 243–249.

© Meteoritical Society • Provided by the NASA Astrophysics Data System